

***Ab initio* coupled-cluster calculations for the fcc and hcp structures of rare-gas solids**

Krzysztof Rościszewski

Institute of Physics, Jagellonian University, Reymonta 4, Pl 30-059 Krakow, Poland

Beate Paulus and Peter Fulde

Max Planck Institut für Physik Komplexer Systeme, Nöthnitzerstrasse 38, D-01187 Dresden, Germany

Hermann Stoll

Institut für Theoretische Chemie, Universität Stuttgart, D-70550 Stuttgart, Germany

(Received 28 March 2000)

In order to gain more insight into factors governing the relative stability of the fcc and hcp structures of the rare-gas solids Ne through Xe, we performed *ab initio* coupled-cluster calculations for the most important three- and four-body terms in the many-body expansion of the cohesive energy. These terms are combined with empirical two-body potentials derived from dimer data and with a multipole expansion for the long-range three-body terms. In addition, we calculated phonon spectra, in harmonic approximation, for the two structures. Including zero-point energies, our results agree very well with experimental data for the fcc structure. The hypothetical hcp structure, which is lower in energy with two-body potentials, is destabilized by short-range three-body terms and, even more important, by the contribution of zero-point vibration.

I. INTRODUCTION

The theoretical prediction of the lattice structure of the heavier rare-gas solids (neon, argon, krypton, and xenon) has been a long-debated issue. Earlier calculations favored the hexagonal close-packed (hcp) structure whereas experimentally only the face-centered cubic (fcc) one was observed (cf. Ref. 1 and references cited therein). Just a few years ago, two groups claimed, on the basis of a three-atom perturbation analysis,^{2,3} that nonadditive short-range exchange contributions are responsible for the stability of the fcc structure. In a very recent paper, applying relativistic pseudopotentials in a valence *ab initio* coupled-cluster treatment,⁴ we documented the importance of three-body terms for cohesive energies and lattice constants of the rare-gas crystals Ne-Xe. We now want to extend the latter treatment, which was done for the fcc structure, by investigating the relative importance of three-body terms for hcp, at the same level of approximation.

The largest part of the cohesive energy of rare-gas crystals is due to two-body interactions dominated by the van der Waals term $-C/r^6$. For these two-body terms, highly accurate analytic model potentials are available whose coefficients were fitted to experimental data of rare-gas dimers.⁵⁻⁹ These two-body potentials marginally favor the hcp structure. Three-body contributions can be separated into a short-range part, where the Pauli repulsion is non-negligible, and into a long-range part, where only dispersion effects are important. It is for the first one that we perform *ab initio* calculations, at the coupled-cluster level, with single and double excitations and perturbatively including triples [CCSD(T)]. For the latter part, we apply a multipole expansion with a leading induced-dipole term¹⁰ and some of the higher interactions.¹¹⁻¹³ We also include the leading short-range four-body term, calculated at the CCSD(T) level. For the weakly bound rare-gas crystals, the zero-point vibrational energy (ZPE) cannot be neglected; we calculate the ZPE di-

rectly from phonon spectra which, in turn, are determined from the static two-body potentials, in a harmonic approximation. Taking all these contributions into account, we report cohesive energies and lattice constants, both for the experimental fcc structure and for the hypothetical hcp one, as well as bulk moduli for the fcc structure.

The paper is organized as follows: In Sec. II we explain the methods used for the different contributions in more detail. In Sec. III we present and discuss the results obtained for the two structures. Conclusions follow in Sec. IV.

II. METHODOLOGY

Interaction energies per atom are calculated, as functions of the lattice constant a , according to

$$E(a) = E^{(2)}(a) + E^{(3)}(a) + E^{(4)}(a) + E_{\text{ZPE}}(a). \quad (1)$$

Here, the $E^{(n)}$ are static electronic n -body contributions defined as in Ref. 4, and E_{ZPE} is the zero-point energy.

A. Two-body contributions

The two-body contributions, which are derived from dimer data, cover the main part of the cohesive energy of the rare-gas solids. Thus relatively small errors in this part may result in large absolute errors when compared to experiment. In Table I, we list our *ab initio* results of Ref. 4 obtained at the CCSD(T) level using scalar-relativistic pseudopotentials and [7s7p]6d5f4g valence basis sets, together with results obtained with model potentials fitted to experimental data. Although the basis sets used are quite elaborate, the *ab initio* two-body potentials yield only between 92 and 95 % of the ‘‘experimental’’ two-body contributions to the cohesive energy. In order to eliminate these errors we will base all subsequent data on the empirical two-body model potentials of the HFD- B type,⁶⁻⁹ which have been published for all the

TABLE I. *Ab initio* vs empirical two-body contributions to cohesive energies (in μH) determined at the following lattice constants: 4.299 Å (Ne), 5.255 Å (Ar), 5.631 Å (Kr), 6.110 Å (Xe).

	Ne	Ar	Kr	Xe
$E_{ab\text{ initio}}^{(2)}$	-999.0	-3224.3	-4490.6	-6474.24
$E_{\text{emp}}^{(2)}$	-1050.3	-3498.8	-4878.0	-6818.3
$E_{\text{emp}}^{(2)}$		-3490.4		

^aReferences 6–9.

^bReference 5.

rare gases considered in this work. In addition, for Ar we perform calculations with the more recent model potential of Ref. 5. We add up all pair contributions in a sphere of about 750 000 atoms which corresponds to a spherical cutoff of $50a_{\text{fcc}}$; the truncation error is below $0.05\ \mu\text{H}$. The difference between the HFD-*B* and Ref. 5 model-potential results for argon may serve as an estimate of the overall accuracy of these potentials; it is below $10\ \mu\text{H}$, i.e., 0.3% of the two-body cohesive energy.

B. Short-range three-body contributions

In the range where both Pauli repulsion and van der Waals-type interactions are important accurate *ab initio* calculations are required. We hence performed CCSD(T) calculations for all trimer configurations occurring in the crystal lattice, with two (or three) side lengths equalling the nearest-neighbor distance. (For the fcc structure, four such trimers exist, with angles of 60, 90, 120, and 180°, respectively, while for the hcp lattice two additional ones occur with angles of 109 and 146°.) All calculations were done using the MOLPRO-96 program package;¹⁴ scalar-relativistic pseudopotentials¹⁵ were employed for simulating the Rg^{8+} cores (supplemented by a core-polarization potential in the case of Xe), and various valence basis sets were tested, cf. below. The three-body contributions to the crystal cohesive energy were extracted from the trimer results applying counterpoise corrections¹⁶ for basis-set superposition errors (BSSE), as described in detail in Ref. 4.

Let us now consider the influence of the correlation level and of the one-particle basis set on the computed three-body interaction terms. It turns out that the contribution of triple excitations in the coupled-cluster correlation treatment [CCSD(T) vs CCSD] is substantial. At the experimental lattice constant a_{exp} the contribution of triples amounts to about 15% of the total short-range three-body terms, at smaller distances ($\sim 0.9a_{\text{exp}}$) the percentage is even higher (30%).

TABLE II. The leading two-body and three-body terms (in μH) calculated at the experimental lattice constant using different valence basis sets. BF stands for bond-midpoint functions.

Basis set	Ne		Ar		Kr		Xe	
	two-body	three-body	two-body	three-body	two-body	three-body	two-body	three-body
$[5s5p]4d2f$	-101.03	1.74	-334.38	13.84	-424.55	22.14	-645.47	32.39
$[7s7p]6d5f4g$	-126.44	1.86	-414.09	14.28	-576.10	23.92	-831.47	35.64
$[5s5p]4d2f+(1s1p1d)$ BF	-123.91	1.87	-412.80	14.26	-578.36	23.89	-834.68	35.59
Model potential ^a	-131.73		-453.61		-637.48		-893.83	

^aReferences. 6–9.

This shows that the choice of a high-level correlation method is critical for obtaining reliable results.

In order to check requirements for basis-set quality, we performed a series of test calculations for the dimer and the equilateral trimer, with bond lengths fixed at nearest-neighbor distances of the crystal at a_{exp} (see Table II). We start with a contracted $[5s5p]4d2f$ basis set (basis B of Ref. 4), which will be our reference basis set. It goes without saying that counterpoise corrections for BSSE are essential. (Not applying them would lead to a tremendous overbinding for the two-body term, of nearly a factor of 2; cf. also Ref. 17 for a systematic study of BSSE effects, in the case of the neon and argon dimer.) In a first step, we add an additional diffuse $1s1p$ set in an even tempered way. The influence is mostly negligible as long as BSSE corrections are included. In a second step, we augment the $[5s5p]4d2f$ basis set by a polarization set consisting of one diffuse f function (even tempered) and one g function [optimized for the dimer; exponents 0.33 (Ne), 0.23 (Ar), 0.204 (Kr), and 0.183 (Xe)]. With this basis set, an increase of 20–30% is obtained for the two-body term, while for the three-body term the increase is $\sim 10\%$, i.e., significantly smaller. Our most extended basis set was the $[7s7p]6d5f4g$ basis set (basis D of Ref. 4). With respect to the previous set, the two-body term still becomes larger in magnitude by $<5\%$ (reaching about 93% of the experimental HFD-*B* value), while the three-body term is slightly reduced.

Another strategy to improve the basis set consists in adding extra functions at bond midpoints.^{18,19} We explored the effect of adding a $1s1p1d$ bond-midpoint set with a common exponent, to our $[5s5p]4d2f$ reference basis; the exponent was optimized for the dimer dissociation energy (Ne: 0.387, Ar: 0.288, Kr: 0.246, and Xe: 0.211). For the two-body term this basis set yields essentially the same value as the large $[7s7p]6d5f4g$ basis. The same holds true for the three-body term, and the increase with respect to the reference basis is below 10% again, in this case.

In order to compare our results with those published by Lotrich and Szalewicz³ for Ar, we performed all-electron test calculations with their basis set,²⁰ i.e., the $[8s5p]2d1f$ set of Ref. 21. This basis yields nearly the same value for the two-body term as our reference basis, but the three-body contribution is by 3% higher than with our most extended basis set.

Summarizing, we can conclude that we miss a non-negligible percentage ($\sim 10\%$) of the three-body energy with our reference basis set (which has been used for the calculations to be discussed below), but the basis-set depen-

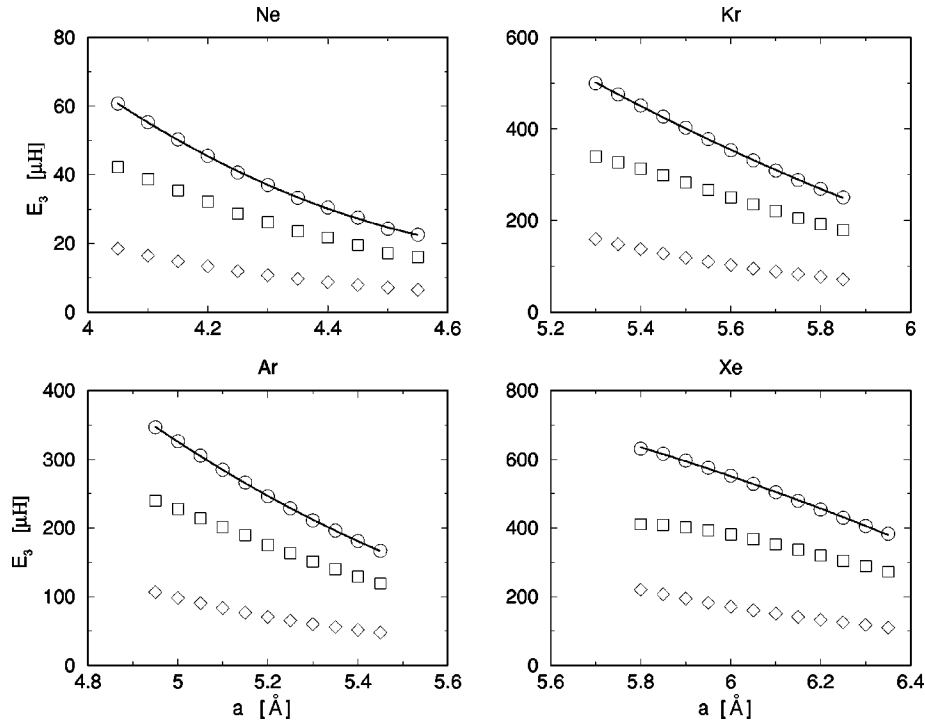


FIG. 1. Three-body contributions to the cohesive energy vs fcc lattice constant (solid line). Both the short-range part (squares) and the long-range part (diamonds) fall approximately linearly with increasing distance.

dence is considerably less pronounced percentage-wise (and much less so in absolute value) than for the two-body energy.

C. Long-range three-body contributions

Three-body contributions from other trimer configurations than those characterized in the previous paragraph are assumed to be purely dispersionlike in our scheme. Although individual magnitudes are very small, the large number of terms leads to a non-negligible total effect. We treat these terms by a multipole expansion, to third-order perturbation theory for ddd , ddq , dqq , qqq , and ddo interactions (d , q , and o stand for dipole, quadrupole, and octopole moments), and add the fourth-order contribution for the leading ddd interaction.¹² The interatomic potential parameters are taken from Ref. 13. For the unknown parameter in the ddo term, we use the lower bound of the values provided by Standard and Certain.²² To achieve convergence in the long-range three-body contribution (changes smaller than 0.1%), we need a sphere of about 6000 atoms. The dependence of both long-range and short-range three-body contributions with the lattice constant a is mainly linearly falling for increasing a (see Fig. 1).

D. Four-body contributions

In order to get an indication of the magnitude of four-body contributions to the cohesion of the rare-gas solids, we calculated the four-body increment of the most compact four-atom cluster occurring in the lattice, i.e., a regular tetrahedron with side length equaling the nearest-neighbor distance. The weight of this increment is the same for fcc and hcp; hence it has no influence on the energy difference between the two structures. We performed CCSD(T) calcula-

tions with the $[5s5p]4d2f$ “reference” basis set and applied the counterpoise correction in an analogous way as for the three-body terms. The numbers obtained are small but non-negligible, and there is a strong dependence on the lattice constant. Since the curvature is negative, this leads to a decrease of the bulk modulus. The influence on the lattice constant itself, on the other hand, is very small since the maximum contribution comes for a value of the lattice constant near the experimental one.

E. Zero-point vibrational energy

The rare-gas solids are weakly bound systems where the zero-point vibrational energy (ZPE) cannot be neglected. If the dynamical properties of the crystal are described within the harmonic approximation, it is easy to define the zero-point crystal energy (per rare-gas atom) as sum of the individual frequencies of the independent oscillators:

$$E_{\text{ZPE}} = \frac{1}{2rN} \sum_{\mathbf{k}, j} \hbar \omega_j(\mathbf{k}) = \frac{3}{2} \hbar \int_0^\infty \omega g(\omega) d\omega. \quad (2)$$

In the first expression, \mathbf{k} is the wave vector and j enumerates phonon branches; r numbers the different atoms in the unit cell, and N is the number of wave vectors in the Brillouin zone (BZ). The second formula corresponds to a continuous description using the frequency distribution function $g(\omega)$. For $g(\omega)$ two approximations are often used: The Einstein approximation replaces $g(\omega)$ by a δ function, which simulates the motion of a single atom in the field of its neighbors.²³ The Debye approximation substitutes $g(\omega) \approx \omega^2$ with a cutoff ω_D to keep the integral finite; this results in a zero-point energy of $\frac{9}{8} k_B T_D$ where T_D is the experimental Debye temperature.²⁴ The Einstein approximation has the

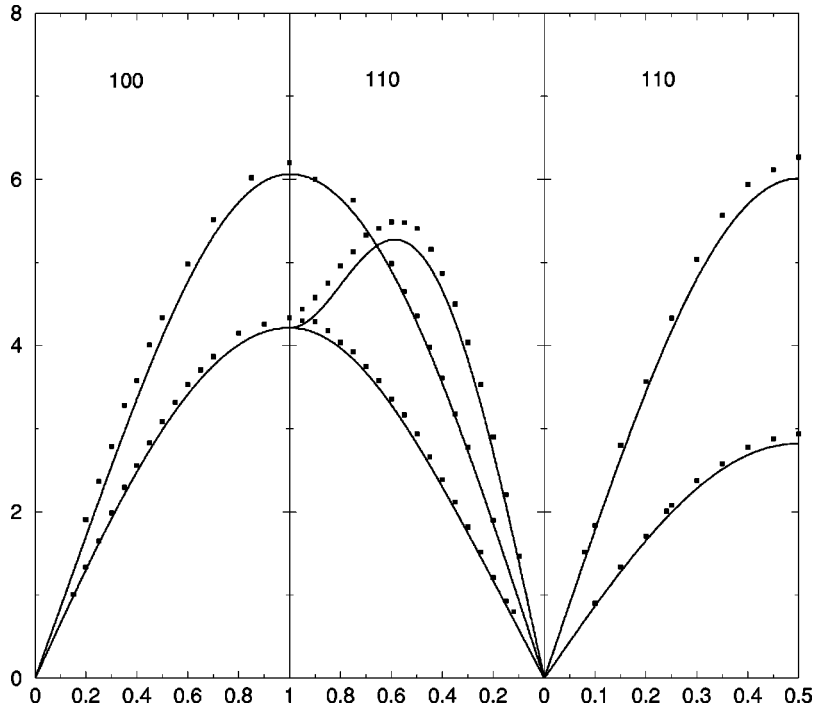


FIG. 2. Harmonic phonons of the fcc krypton lattice computed with the HFD-*B* two-body potential at the lattice constant $a = 5.646 \text{ \AA}$ (solid line). The energy is given in meV and the \mathbf{k} vectors as fractions of $2\pi/a_{\text{fcc}}$. The squares show the experimentally measured phonons (Ref. 28).

advantage that anharmonic effects can be included (quasi-harmonic treatment,²⁵) but, of course, neither the harmonic nor the anharmonic parts are exact.

We stick to the first expression of Eq. (2), i.e., we refrain from imposing some *a priori* assumption on the frequency distribution. However, for the explicit determination of the phonon branches, the harmonic approximation is implied and only contributions from the two-body model potentials are used. For a ZPE determination accurate to $0.05 \mu\text{H}$ it is sufficient to include the interaction between about 8000 atoms. This is a much smaller value than for the two-body energy due to the rapid decrease of the derivatives of the two-body potential and the weighting of these terms with a cosine prefactor in the dynamical matrix. The \mathbf{k} grid is chosen to be homogeneous in the BZ avoiding the coincidence with special points and directions. Again, the number of \mathbf{k} points is chosen so large that the concomitant error in the ZPE is below $0.05 \mu\text{H}$. Comparing our results for fcc rare-gas crystals with the measured phonon spectrum,^{26–29} we find reasonable agreement for all branches (see the krypton results in Fig. 2); just the magnitude of the phonons is too large, by up to 15% for neon, which is consistent with the estimates for the anharmonic effects and the influence of three-body terms.³⁰ Plotting the hcp phonons in the 010 and 001 direction (see Fig. 3 for krypton), we find the expected branches as observed, e.g., for hcp metals or the hcp helium crystal.

III. RESULTS AND DISCUSSION

A. Ground-state properties of the fcc rare-gas solids

For the experimentally observed fcc structure, we determined the cohesive energy, the lattice constant and the bulk

modulus. In Table III we present different contributions to the cohesive energy evaluated at the experimental lattice constant. It is seen that the static two-body contribution overestimates the binding energy by between 12% for xenon and 30% for neon. Including the (repulsive) three-body contributions, this overbinding is reduced. While for neon the effect is small (only 3% of the cohesive energy), its importance rises for the heavier rare-gas solids to $\sim 8\%$ (for xenon). The short-range part amounts to about 70% of the three-body contribution. A purely multipolar description of the three-body potential severely underestimates it, yielding only 10% of the short-range part compared with the *ab initio* results. The four-body contribution is small (between 0.4% for neon and 1.0% for xenon), but its importance increases for the heavier rare gases. The zero-point energy is repulsive, too, of course. It amounts to 30% of the cohesive energy for neon, 10% for argon, 5% for krypton, and 3% for xenon. We esti-

TABLE III. The influence of different contributions (as defined in Sec. II) to the cohesive energy (in μH) for the fcc structure at the experimental lattice constant.

	Ne	Ar	Kr	Xe
$E^{(2)}$	-993.4	-3464.2	-4840.6	-6799.1
$E_{\text{s.r.}}^{(3)}$	18.9	148.6	230.1	343.0
$E_{\text{l.r.}}^{(3)}$	7.7	59.4	93.0	145.1
$E^{(4)}$	3.2	24.9	38.9	58.9
E_{ZPE}	212.7	288.3	214.7	200.1
E_{coh}	-750.9	-2943.0	-4263.9	-6052.0
E_{exp}	-752.2 ^a	-2943.9 ^b	-4264.3 ^b	-6051.2 ^b

^aReference 33.

^bReference 34.

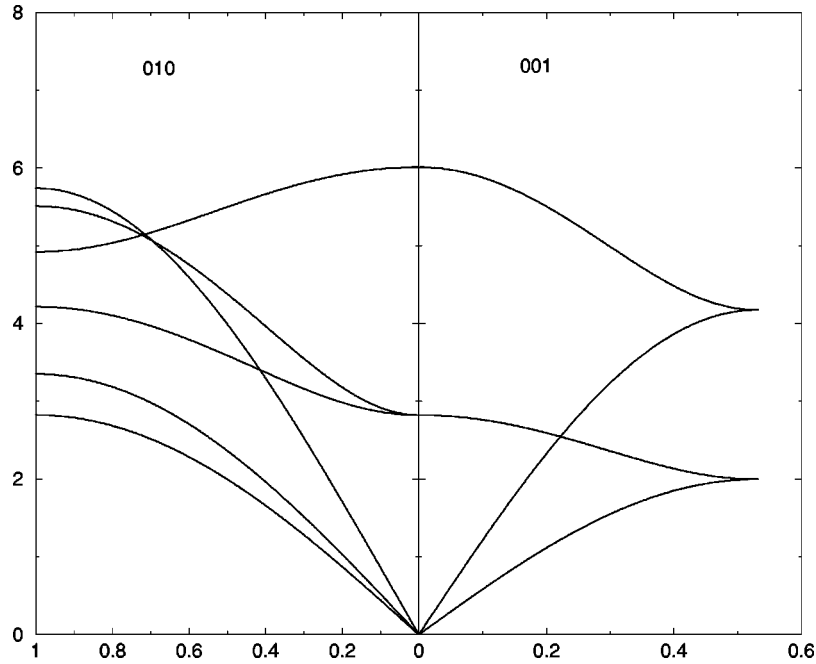


FIG. 3. Harmonic phonons of the hypothetical hcp krypton lattice computed with the HFD-*B* two-body potential at the lattice constant $a = 5.646 \text{ \AA}$ (solid line). The energy is given in meV and the \mathbf{k} vectors as fractions of $2\pi/a_{\text{hcp}}$.

mate the error of the calculated zero-point energy to $\sim 15\%$, due to the missing three-body contributions and anharmonicity effects; this is our main source of error. The error bar for the two-body contributions is $\sim 0.3\%$ (cf. Sec. II A), and $\sim 10\%$ for the short-range three-body contribution (due to the finite basis sets used). About the same (absolute) error can be expected to arise from the neglect of further four-body contributions. (Note that our value listed in Table III is a lower bound to the total four-body contributions, since we calculated only the largest increment.) Overall we have to deal with a maximum error of $\pm 5\%$ for the cohesive energy. Comparing our results with experiment, we find much smaller deviations ($\pm 0.5\%$) indicating rather efficient error cancellation.

In the next step, we calculated the fcc lattice constant (see Table IV). The two-body contribution leads to a sizable underestimation of the lattice constant (by up to 4% for neon). Higher-body terms enlarge the lattice constant only slightly (largest effect for xenon: $+0.6\%$), whereas the zero-point energy yields a significant increase. Taking all contributions into account, our calculated values agree well with the experimental ones (deviation $< 0.7\%$).

The bulk modulus (see Table V) calculated at the theoretical equilibrium lattice constant, for each of the different levels of approximation, is strongly overestimated at the two-body level (by up to a factor of 2). For neon, the main reduction is due to the zero-point energy whereas for the heavier rare-gas solids the effect is a mixture of many-body contributions and zero-point energy. Our final result agree within $\pm 10\%$ with the experimental data, which by themselves have uncertainties of the same magnitude.

B. Comparison between the fcc and hcp structure

Table VI shows energy differences between the fcc and hcp structures calculated at the different levels of approxi-

mation for the corresponding equilibrium lattice constants. (The optimization of the hcp lattice constants always yields the same nearest-neighbor distances as for the corresponding fcc ones, to $< 1 \times 10^{-3} \text{ \AA}$). The two-body contribution slightly favors the hcp structure. The corresponding fcc-hcp energy difference is not very sensitive to the value of the lattice constant where it is determined (see lines 1 and 2 in Table VI). For Ar, we can also compare the result obtained with the HDF-*B* potential to the one with the potential of Ref. 5. We get virtually the same numbers ($0.43 \mu\text{H}$ vs $0.44 \mu\text{H}$). On the other hand, Lotrich and Szalewicz³ report a value of only $0.1 \mu\text{H}$ with the potential of Ref. 5. We can only guess that the deviation is due to the smaller number of atoms taken into account. (About 8000 atoms in a cube are used in Ref. 3, as compared to a sphere of 750 000 atoms in our case, and the absolute value of the two-body energy for the fcc structure is by $0.67 \mu\text{H}$ smaller than ours.)

TABLE IV. The influence of different contributions to the lattice constant of the fcc structure (in \AA). The energy terms of Table III are consecutively included.

	Ne	Ar	Kr	Xe
$a^{(2)}$	4.277	5.213	5.556	6.054
$a^{(+3,\text{s.r.})}$	4.290	5.239	5.584	6.076
$a^{(+3,\text{l.r.})}$	4.296	5.249	5.597	6.088
$a^{(+4)}$	4.297	5.251	5.598	6.087
$a^{+\text{ZPE}}$	4.468	5.311	5.633	6.111
a_{exp}	4.464 ^a	5.311 ^b	5.670 ^c	6.132 ^d

^aReference 35.

^bReference 36.

^cReference 37.

^dReference 38.

TABLE V. The influence of different contributions to the bulk modulus of the fcc structure (in kbars). The energy terms of Table III are consecutively included.

	Ne	Ar	Kr	Xe
$B^{(2)}$	19.9	37.5	41.7	46.2
$B_{s.r.}^{(+3)}$	19.2	34.4	37.8	41.3
$B_{l.r.}^{(+3)}$	18.8	33.6	36.9	40.4
$B^{(+4)}$	18.8	33.1	36.1	39.6
B^{+ZPE}	10.4	27.9	32.9	37.2
B_{exp}	10.9 ^a	26.7 ^b	36.1 ^c	36.4 ^d

^aReference 26.

^bReference 39.

^cReference 28.

^dReference 29.

The short-range three-body contributions favor the fcc structure, but would render it stable only for xenon, in our calculations. Taking into account the long-range contributions, too, which favor hcp again, the net effect of the three-body contributions is almost zero. This is in contradiction to the values published by Lotrich and Szalewicz³ (LS) for argon. Although the total amount of the three-body contributions (LS: 217 μ H, this work: 223 μ H) and the hcp-fcc differences obtained with our short-range three-body contributions (0.35 μ H) and those of LS (0.32 μ H) agree well, there is a sizable deviation due to the long-range contributions. Whereas we adopted empirical parameters from literature, Lotrich and Szalewicz³¹ used interaction parameters fitted to their *ab initio* data.

In our calculations, the largest contribution to the hcp-fcc difference comes from the zero-point energy. The latter favors the fcc structure by about 1–3 μ H, which corresponds to about 1% of the zero-point energy. Previous calculations applying a simpler two-body potential³² and the Einstein approximation obtained a much smaller difference (0.01% of the zero-point energy). For Ar, LS (Ref. 3) included the effect of anharmonicity and of three-body terms to the ZPE, in the Einstein approximation, but still the stabilizing effect for the hcp structure was below 0.1 μ H. In total, we find the experimentally observed fcc structure to be lower in energy than the hcp one for all rare-gas crystals considered (as LS for Ar), but our energy difference for Ar is by about an order of magnitude larger (2.8 vs 0.3 μ H) and due to different reasons than in the work of LS.

TABLE VI. The energy difference between the fcc and hcp structures (in μ H) evaluated at equilibrium lattice constants optimized for the various levels of approximation. The numbers in the parentheses are calculated at the experimental lattice constant.

	Ne	Ar	Kr	Xe
two-body	+0.13 (+0.10)	+0.43 (+0.38)	+0.61 (+0.53)	+0.85 (+0.73)
three-body s.r.	−0.08	−0.35	−0.53	−1.03
three-body l.r.	+0.03	+0.32	+0.54	+0.56
ZPE	−1.08	−3.24	−2.64	−2.72
Total	−1.00	−2.84	−2.023	−2.34

IV. CONCLUSION

We have determined ground-state properties of the rare-gas solids Ne through Xe, by combining empirical and *ab initio* based theoretical data. For the two-body contributions $E^{(2)}$, we applied accurate empirical model potentials derived from dimer data. Three-body contributions $E^{(3)}$ were treated separately, with respect to short-range and long-range terms. For the first ones, we performed *ab initio* calculations at the CCSD(T) level, while the long-range part was evaluated using a multipole expansion. In addition, a first estimate has been obtained for the four-body contributions, which turned out to be non-negligible for the heavier rare-gas solids. Finally, the zero-point energy E^{ZPE} has been calculated via the harmonic phonon spectrum derived from the two-body model potential.

All these contributions are essential for the accurate determination of the cohesive energy E_{coh} , the lattice constant a , and the bulk modulus B . For the (experimental) fcc structure we achieve agreement with experiment to ~ 2 μ H for E_{coh} , 0.04 \AA (0.7%) for a , and 3 kbars (10%) for B . For neon, the zero-point energy is by far the most important correction to $E^{(2)}$, whereas for the heavier compounds the many-body contributions gain in weight, with $E^{(3)}$ exceeding E^{ZPE} for krypton and xenon.

The fcc structure is favored energetically over the hcp one by the combined effect of short-range three-body terms and the zero-point vibrational energy; the main contribution comes from ZPE, in our calculations, which is in contrast to previous estimates using the Einstein approximation. In view of the importance of dynamics, further investigations focusing on contributions of three-body potentials and anharmonic terms to the phonon spectra appear to be called for.

¹Rare Gas Solids, edited by M.L. Klein and J.A. Venables (Academic Press, London, 1970), Vol. I.

²G. Dotelli and L. Jansen, Physica A **234**, 151 (1996).

³V.F. Lotrich and K. Szalewicz, Phys. Rev. Lett. **79**, 1301 (1997).

⁴K. Rosciszewski, B. Paulus, P. Fulde, and H. Stoll, Phys. Rev. B **60**, 7905 (1999).

⁵R.A. Aziz, J. Chem. Phys. **99**, 4518 (1993).

⁶R.A. Aziz and M.J. Slaman, Chem. Phys. **130**, 187 (1989).

⁷R.A. Aziz and M.J. Slaman, J. Chem. Phys. **92**, 1030 (1990).

⁸A.K. Dham, A.R. Allnatt, W.J. Meath, and R.A. Aziz, Mol. Phys. **67**, 1291 (1989).

⁹A.K. Dham, W.J. Meath, A.R. Allnatt, R.A. Aziz, and M.J. Slaman, Chem. Phys. **142**, 173 (1990).

¹⁰B.M. Axilrod and E. Teller, J. Chem. Phys. **11**, 299 (1943).

¹¹R.J. Bell, J. Phys. B **3**, 751 (1970).

¹²M.B. Doran and I.J. Zucker, J. Phys. C **4**, 307 (1971).

¹³G. Marcelli and R.J. Sadus, J. Chem. Phys. **111**, 1533 (1999).

¹⁴MOLPRO is a package of *ab initio* programs written by H.J. Werner and P.J. Knowles with contributions from J. Almlöf, R.D. Amos, M.J.O. Deegan, S.T. Elbert, C. Hampel, W. Meyer, K. Peterson, R. Pitzer, A.J. Stone, and P.R. Taylor; C. Hampel, K. Peterson, and H.-J. Werner, Chem. Phys. Lett. **190**, 1 (1992);

- M.J.O. Deegan and P.J. Knowles, *ibid.* **227**, 321 (1994).
- ¹⁵A. Nicklass, M. Dolg, H. Stoll, and H. Preuss, *J. Chem. Phys.* **102**, 8942 (1995).
- ¹⁶S.F. Boys and F. Bernardi, *Mol. Phys.* **19**, 553 (1970).
- ¹⁷T. van Mourik, A.K. Wilson, and T.H. Dunning, Jr., *Mol. Phys.* **96**, 529 (1999).
- ¹⁸H.L. Williams, E.M. Mas, K. Szalewicz, and B. Jeziorski, *J. Chem. Phys.* **103**, 7374 (1995).
- ¹⁹F.-M. Tao, *J. Chem. Phys.* **111**, 2407 (1999).
- ²⁰V.F. Lotrich, H.L. Williams, K. Szalewicz, B. Jeziorski, R. Moszynski, P.E.S. Wormer, and A. van der Avoird, *J. Chem. Phys.* **103**, 6076 (1995).
- ²¹H. Partridge and K. Faegri, Jr., *Theor. Chim. Acta* **82**, 207 (1992).
- ²²J.M. Standard and P.R. Certain, *J. Chem. Phys.* **83**, 3002 (1983).
- ²³A.A. Maradudin, in *Dynamical Theory of Solids*, edited by G.K. Horton and A.A. Maradudin (North Holland, Amsterdam, 1974), Vol. I.
- ²⁴B. Farid and R. Godby, *Phys. Rev. B* **43**, 14 248 (1991).
- ²⁵M.L. Klein and T.R. Koehler, in *Rare Gas Solids* (Ref. 1).
- ²⁶Y. Endoh, G. Shirane, and J. Skalyo, Jr., *Phys. Rev. B* **11**, 1681 (1975).
- ²⁷Y. Fujii, N.A. Lurie, R. Pynn, and G. Shirane, *Phys. Rev. B* **10**, 3647 (1974).
- ²⁸J. Skalyo, Jr., Y. Endoh, and G. Shirane, *Phys. Rev. B* **9**, 1797 (1974).
- ²⁹N.A. Lurie, G. Shirane, and J. Skalyo, Jr., *Phys. Rev. B* **9**, 5300 (1974).
- ³⁰R.J. Bell, and I.J. Zucker, in *Rare Gas Solids* (Ref. 1).
- ³¹V.F. Lotrich and K. Szalewicz, *J. Chem. Phys.* **106**, 9688 (1997).
- ³²C. Isenberg and C. Domb, in *Lattice Dynamics*, edited by R.F. Wallis (Pergamon, New York, 1995), p. 141.
- ³³G.J. McConville, *J. Chem. Phys.* **60**, 4093 (1974).
- ³⁴L.A. Schwalbe, R.K. Crawford, H.H. Chen, and R.A. Aziz, *J. Chem. Phys.* **66**, 4493 (1977).
- ³⁵D.N. Batchelder, D.L. Losee, and R.O. Simmons, *Phys. Rev.* **162**, 767 (1967).
- ³⁶O.G. Peterson, D.N. Batchelder, and R.O. Simmons, *Phys. Rev.* **150**, 703 (1966).
- ³⁷D.L. Losee and R.O. Simons, *Phys. Rev.* **172**, 944 (1968).
- ³⁸D.R. Sears and H.P. Klug, *J. Chem. Phys.* **37**, 3002 (1962).
- ³⁹S. Gewurtz and P. Stoicheff, *Phys. Rev. B* **10**, 3487 (1974).